Available online at www.sciencedirect.com
SCIENCE DIRECT®
Developmental Biology 283 (2005) 424 – 436
DEVELOPMENTAL BIOLOGY
www.elsevier.com/locate/ydbio

The genetic and molecular analysis of *spe-19*, a gene required for sperm activation in *Caenorhabditis elegans*

Brian Geldziler, Indrani Chatterjee, Andrew Singson*

Waksman Institute and Department of Genetics, Rutgers University, 190 Frelinghuysen Road, Piscataway, NJ 08854, USA

Received for publication 28 October 2004, revised 28 April 2005, accepted 28 April 2005
Available online 4 June 2005

Abstract

During the process of spermiogenesis (sperm activation) in *Caenorhabditis elegans*, the dramatic morphological events that ultimately transform round sessile spermatids into polar motile spermatozoa occur without the synthesis of any new gene products. Previous studies have identified four genes (*spe-8*, *spe-12*, *spe-27* and *spe-29*) that specifically block spermiogenesis and lead to hermaphrodite-specific fertility defects. Here, we report the cloning and characterization of a new component of the sperm activation pathway, *spe-19*, that is required for fertility in hermaphrodites. *spe-19* is predicted to encode a novel single-pass transmembrane protein. The *spe-19* mutant phenotype, genetic interactions and the molecular nature of the gene product suggest SPE-19 to be a candidate for the receptor/co-receptor necessary for the transduction of the activation signal across the sperm plasma membrane.

Keywords: Fertilization; Sperm; Spermiogenesis; Spermatogenesis; *C. elegans*

Introduction

Differentiating cells typically undergo dramatic morphogenetic changes to form and maintain structures crucial for the initiation and maintenance of that differentiation. For most studied cell types, this usually involves the synthesis of new and specialized gene products (Blau, 1992; Chandrasekhar et al., 1992; Finney et al., 1987; Kraft et al., 1989; Shapiro, 1985; Simon et al., 1991; Simons and Fuller, 1985; Simons and Wandinger-Ness, 1990). In some cell types, however, morphological change is known to occur in the absence of any new macromolecular synthesis. Anucleate platelets, for example, differentiate rapidly during blood clotting, accomplished primarily via actin cytoskeleton alterations (Derenlau, 1987; Nachmias et al., 1987). Egg cortical granule fusion via calcium-calmodulin signaling and the sperm acrosome reaction serve as other well-known examples (Primakoff and Myles, 2002; Vacquier, 1975; Wassarman et al., 2001). The nematode *Caenorhabditis elegans* serves as an ideal model organism to examine cellular differentiation and morphogenesis via post-translational modification, as *C. elegans* sperm synthesize no new mRNA or protein (indeed, they contain no ribosomes), yet complete a remarkable morphological transformation from spermatid to spermatozoa (Geldziler et al., 2004; L'Hernault, 1997; L'Hernault and Singson, 2000; Singson, 2001).

Spermiogenesis in *C. elegans* is a rapid process, typically taking less than 5 min to complete (Nelson and Ward, 1980). Although its onset differs between males and hermaphrodites (hermaphrodite spermatids undergo activation after entry into the spermatheca, while males undergo activation soon after ejaculation into the uterus), the events are similar regardless of sperm derivation. Upon exposure to an unidentified activation signal, round sessile spermatids begin to polymerize filaments of Major Sperm Protein (MSP), which then coalesce to form the dynamic cytoskeleton and polar pseudopod needed by the sperm for motility

* Corresponding author. Fax: +1 732 445 5735.
E-mail address: singson@waksman.rutgers.edu (A. Singson).

0012-1606/$ - see front matter © 2005 Elsevier Inc. All rights reserved.
doi:10.1016/j.ydbio.2005.04.036

and thus fertilization competence. On the opposite side of the cell, novel structures called membranous organelles (MO) fuse with the plasma membrane (Achanzar and Ward, 1997; L'Hernault, 1997; Shakes and Ward, 1989a; Singson, 2001). The function of these MOs and their fusion is not known.

Mutations in four genes, *spe-8*, *spe-12*, *spe-27* and *spe-29*, specifically affect this process of spermiogenesis in hermaphrodites, leading to a hermaphrodite-specific fertility defect in these animals. Available genetic and phenotypic evidence suggests that *spe-8*, *spe-12*, *spe-27*, *spe-29* and *spe-6* act in a common pathway (Muhlrad and Ward, 2002; Nance et al., 1999, 2000). Here, we present a phenotypic, genetic and molecular analysis of a new gene, *spe-19*, that is required for spermiogenesis in hermaphrodites but not males in vivo and whose mutants share the general *spe-8* class phenotype. We have cloned *spe-19*, which is predicted to encode a novel 300 amino acid type 1 transmembrane protein.

Materials and methods

Worm culture and strains

All strains used were maintained on *Escherichia coli OP50*-seeded NGM plates and manipulated as previously described (Brenner, 1974). The *C. elegans* Bristol strain N2 is considered wild-type, and the following mutants were also used in this study: *spe-8(hc53) dpy-5(e61)*, *spe-6(hc163), spe-8(hc40), dpy-18(e364)*, *dpy-21(e428)*, *unc-76(e911)*, *unc-51(e1189)*, *rol-9(sc149)*, *him-5(e1490), dpy-5(e61)*, *fog-2(q71)*, *fer-1(hc1ts)*, *fem-1(hc17)*, ozDF1/*sdc-3(y52y180), unc-76(e911)*V, ozDF2/*dpy-21(e428), par-4(it33)*V, yDF4/*dpy-11(e224)*, *unc-76(eq11)*V. The Hawaiian strain CB4856 was used for SNP mapping. *spe-19(hc41)* was isolated from a sperm development screen in the Ward laboratory (Shakes, 1988), and *spe-19(eb52)* was isolated from an ethylmethanosulfate (EMS) mutagenesis conducted by Mako Saito and Tim Schedl. *spe-6(h163)* worms were provided by Paul Muhlrad and Sam Ward. All other strains were provided by the CGC. Descriptions of all mutants used in this study may be found in Hodgkin (1997).

Worm genetics

spe-19 was mapped using a combination of standard two-point, three-point, deficiency and snip-SNP techniques (Jakubowski and Kornfeld, 1999). *spe-19* lies on the far right of Chromosome V (Fig. 6A). Three-point mapping using *dpy-21* and *rol-9* gave two recombinant classes, suggesting that *spe-19* lies between the two genes and closer to *rol-9* (Rol non-Dpy: 5/132 Spe, Dpy non-Rol 4/13 Spe).

Two-point data using *dpy-21 spe-19* recombinants generated from the above three-point mapping experiment suggested that *spe-19* lies approximately 11.4 MU to the right of *dpy-21* at approximately position 24.6 (16/70 Dpy Spe).

Of the three deficiencies in the *spe-19* region, *spe-19(eb52)* and *spe-19(hc41)* complement yDF4(V) and fail to complement ozDF1(V), consistent with the above mapping data (Fig. 6A). Importantly, *spe-19*/ozDF1 worms exhibit no additional phenotypes, suggesting that sterility is the null phenotype. Interestingly, *spe-19* also complemented ozDF2(V) whose predicted right end lies at map position 25.12, suggesting that perhaps this deficiency is complex.

unc-76; spe-19 and *spe-19; rol-9* double mutants were created and used for snip-SNP mapping. These worms were first crossed into Hawaiian strain CB4856, and their progeny allowed to self-fertilize. Recombinants were then picked and assayed for the presence of single nucleotide polymorphisms. Snip-SNP mapping using these *unc-76* non-*spe-19* (n = 48) and *rol-9* non-*spe-19* (n = 6) recombinants enabled us to map *spe-19* to the ~450 kb interval between cosmids M162 (map position 23.31) and ZC15 (map position 24.95), an interval predicted to contain approximately 100 genes on the far right of chromosome V. A search for candidate genes within the interval suggested Y113G7A.10 as a likely prospect as it is one of two genes in the region whose expression is sperm-enriched (Reinke et al., 2004).

Male lines were generated by first crossing *spe-19/+* males to *spe-19/spe-19* hermaphrodites. Single male progeny were then crossed to *spe-19/spe-19* hermaphrodites, L4 progeny were picked and scored for sterility. *spe-6* suppression experiments were performed as described by Muhlrad and Ward (2002) using the weak hypomorphic allele *spe-6(hc163)*. Homozygous *spe-6, dpy-18* hermaphrodites were mated to either homozygous *spe-19* or *fog-2* (a non-spermiogenesis hermaphrodite-specific sterile control) males. F1 heterozygotes were plated and allowed to self-fertilize. Dpy F2s were then plated and scored for sterility. Approximately one fourth of all Dpy progeny would be expected to be sterile unless this phenotype was suppressed by *spe-6(hc163)*. 0/315 Dpys were sterile when crossed to *spe-19* animals, while 44/179 Dpys were sterile using the *fog-2* control. To ensure that the homozygous *spe-19* class of animals was present, individual Dpy hermaphrodites were then crossed to homozygous *spe-19* males, and progeny were scored for sterility. Animals for whom all progeny were sterile (2 of 16) indicated that the *spe-19* homozygous class of animal was present.

Statistical analyses

Appropriate statistical tests for significance (t test, Mann–Whitney Rank Sum, ANOVA) were performed using SigmaStat (Systat Software, Inc. Point Richmond, CA).

Ovulation/progeny counts

To determine ovulation/progeny numbers, L4 hermaphrodites raised at specific temperatures were individually plated and allowed to self-fertilize. Oocytes/eggs were counted daily, and hermaphrodites were transferred to new plates until no new eggs/oocytes were laid in a 24-h period. Hermaphrodites that died while still containing oocytes/eggs were excluded from the analysis. All errors reported are given as standard error of the mean.

Light microscopy

Sperm development was assessed as previously described (Nelson and Ward, 1980; Shakes and Ward, 1989b) by dissecting testis or spermatheca in pH 7.8 sperm medium (SM) both with and without the known in vitro activators Pronase (Garner et al., 1974) (200 μg/ml) or triethanolamine (120 mM at pH 7.8). To examine sperm cell nuclei, worms were first fixed in cold methanol for 5 min then stained with 0.1 μg/ml of the DNA-binding dye 4, 6-diamidino-2-phenylindole (DAPI) (Pierce, Rockford, IL) and mounted on 2% agarose slides for viewing using both fluorescence and Nomarski imaging. Oocytes were dissected from the uterus, fixed for 3 min in cold methanol, and stained with DAPI for examination.

Sperm competition assays

spe-19 or N2 males were crossed 4:1 to *dpy-5* hermaphrodites and removed after 24 h. The number of both Dpy (self) and Non-Dpy (outcrossed) progeny were then scored as previously described (Singson et al., 1999).

Transactivation assays

spe-19 L4 hermaphrodites were crossed 1:4 to *fer-1; him-5* homozygous males at 25°C, a temperature at which *fer-1* animals are sterile due to a sperm motility defect (Achanzar and Ward, 1997; Shakes and Ward, 1989b). Progeny were then counted for each Spe hermaphrodite.

DNA transformation

We amplified a 7.3 kb genomic fragment from wild-type worms containing the entire putative *spe-19* region (Y113G7A.10) including ~850 bp of upstream sequence using Platinum Taq (Invitrogen, Carlsbad, CA) and the following primer set:

5′ GTTCAAAAGTTATCAGTGGTCAGAA 3′
5′ CACATTTTTAGCCCTTAAACAGC 3′.

Adult N2 hermaphrodites (F_0) were transformed with these PCR products (10 μg/ml) as described by Mello and Fire (1995) using co-injected *myo3*::*gfp* as a transformation marker (100 μg/ml) and allowed to self fertilize. F_1 hermaphrodites containing the transgene (as indicated by GFP fluorescence) were then also allowed to self-fertilize, and stable glowing F_2 hermaphrodites were next crossed into a *spe-19* mutant background. Glowing F_3 *spe-19* heterozygotes were then allowed to self-fertilize, and glowing F_4s were scored for self fertility. To confirm rescue, non-glowing F_5 hermaphrodites were plated and scored for sterility.

Amplification of cDNA

spe-19 cDNA was amplified from a male-derived cDNA library constructed in Sam Ward's laboratory (Achanzar and Ward, 1997) using the following primer set:

5′ ATGCAAATATTCTTCTTGTTC 3′
5′ ATTCCTGCAAGACCGAGTA 3′.

Exon–intron boundaries were determined by sequencing (UMDNJ-RWJMS DNA Core Facility using an ABI Prism 3100 Genetic Analyzer) and subsequent comparison to genomic DNA.

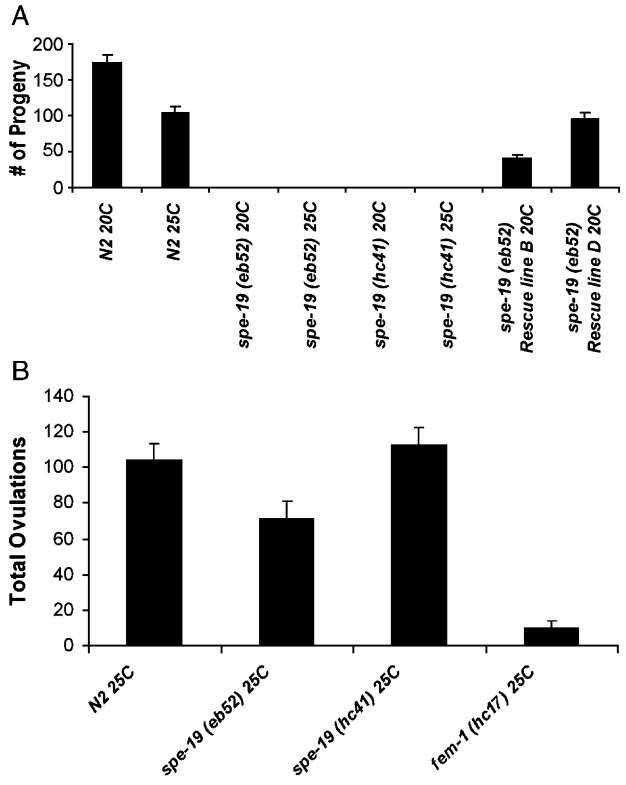

Fig. 1. *spe-19* hermaphrodite fertility. (A) *spe-19* self-fertility. L4 hermaphrodites raised at the indicated temperatures were plated and allowed to self-fertilize. Eggs were counted daily. All error bars represent SEM. (B) Total ovulation counts. L4 hermaphrodites raised at the indicated temperatures were plated and allowed to self-fertilize. Oocytes were counted daily until none were laid in a 24-h period. $n > 15$ for all groups.

Identification of spe-19 molecular lesions

DNA from the putative *spe-19* gene interval was PCR-amplified from genomic DNA of both N2 and each *spe-19* allele. Exons and introns were sequenced completely on both DNA stands to ensure accuracy.

Results

spe-19 hermaphrodites are sterile but ovulate at high levels

There are two independently isolated recessive alleles of *spe-19*. The brood sizes of homozygous *spe-19(eb52)* and

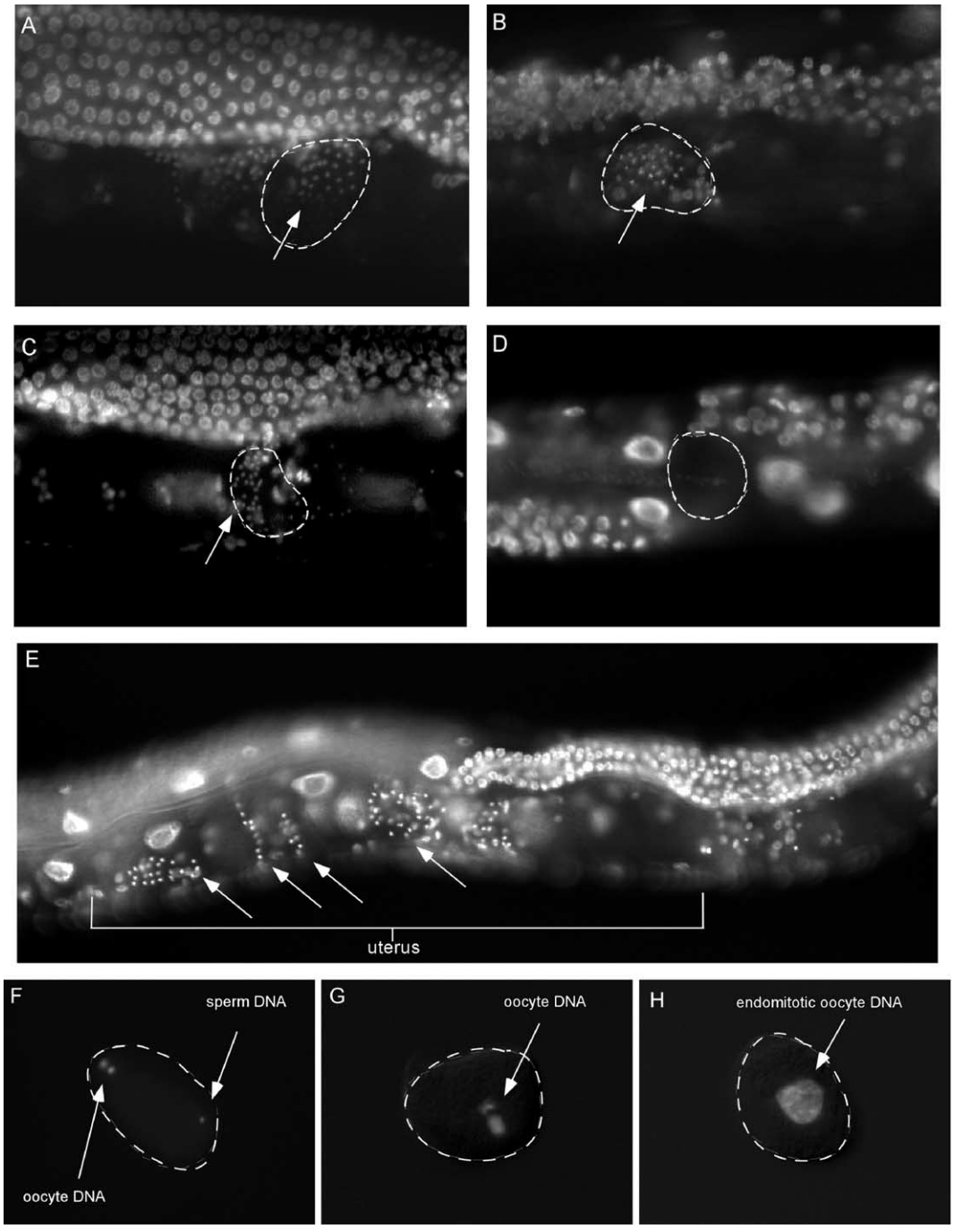

Fig. 2. DAPI sperm loss phenotype; *spe-19* mutant sperm are lost from the reproductive tract and do not penetrate oocytes. DAPI images of age-matched young adult wild-type (A) and *spe-19(eb52*) (B) and older adult (3-day post L4) wild-type (C) and *spe-19(eb52)* animals. The position of the spermatheca is indicated by dashed lines, and spermatid nuclei are visible as small, bright puncta (arrows). (E) Ectopic spermatid presence. Unable to migrate back to the spermatheca after displacement by passing oocytes, spermatids can be found in the uterus and near the vulva of spe-19 hermaphrodites. (F–H) DAPI-stained dissected oocytes. (F) Wild-type; (G) young *spe-19* oocyte; (H) older EMO *spe-19* oocyte. The oocyte outline is indicated by dashed lines.

spe-19(hc41) animals were determined to quantify fertility. At 20°C and 25°C, both alleles were sterile (Fig. 1A). N2 was used as a wild-type control. Total ovulations over the lifetime of *spe-19* animals were also recorded. At 25°C, the number of both *spe-19(hc41)* and *spe-19(eb52)* ovulations were similar to those of wild-type worms and significantly greater than the basal ovulation level as indicated by *fem-1* animals (*hc41* = 112 ± 10, *eb52* = 71 ± 10, N2 = 104 ± 9, and *fem-1* = 10 ± 4, $n > 15$ for all groups; [$P < 0.05$]) (Fig. 1B). It has been shown that spermatids are required to induce high levels of oocyte maturation and ovulation (McCarter et al., 1999; Miller et al., 2001). Therefore, these results suggest that *spe-19* worms, although sterile, still produce spermatids. Additionally, we noted that *spe-19(eb52)* animals did exhibit fewer total ovulations than *spe-19(hc41)* ($P < 0.05$).

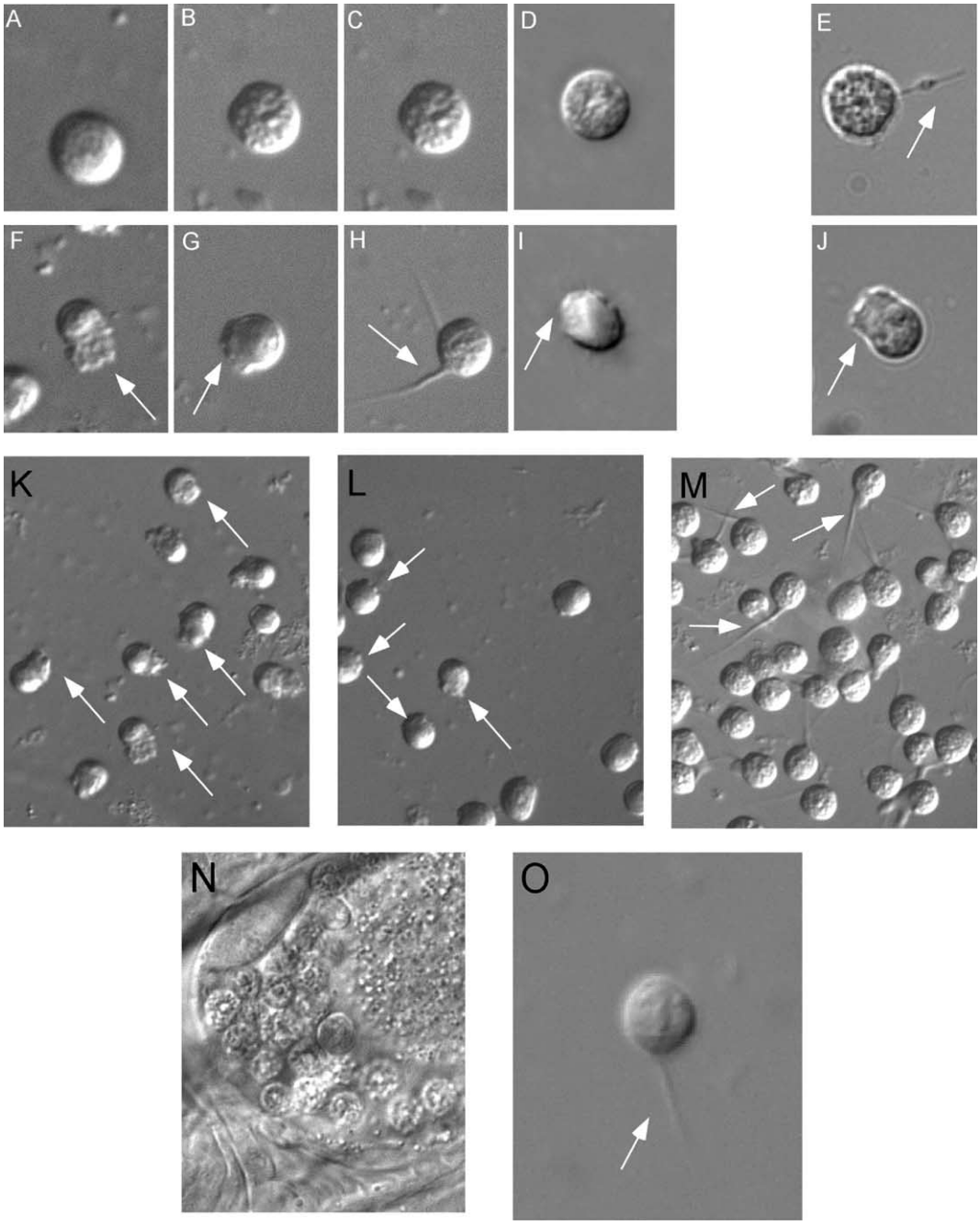

Fig. 3. Sperm activation phenotypes. Spermatids from adult males were dissected in sperm medium (A–D) or sperm medium+Pronase (F–I). (A, F) Wild-type; (B, G) *spe-19(hc41)*; (C, H) *spe-19(eb52);* (D, I) *spe-8(hc40)*. (K–M) Representative sperm fields after Pronase activation. (K) Wild-type; (L) *spe-19(hc41)*; (M) *spe-19(eb52)*. (E, J) TEA sperm activation. (E) *spe-19(eb52)*; (J) *spe-8(hc40)*. (N–O) Spermatids from *spe-19(eb52)* young adult hermaphrodites dissected in sperm medium without (N) or with (O) Pronase. In all panels, arrows indicate pseudopods or spikes.

spe-19 hermaphrodite-derived sperm are prematurely depleted, do not maintain their position in the reproductive tract and fail to enter oocytes

Since the above results suggested the presence of spermatids in *spe-19* animals, we sought to determine any differences in these spermatids from wild-type. Using age-matched DAPI-stained young adult animals raised at 20°C, intact worms were examined under light microscopy to visualize sperm nuclei. Although young adult *spe-19* animals produced comparable amounts of sperm to wild-type (Figs. 2A, B), older adult animals exhibited a marked reduction of visible sperm as compared to wild-type (Figs. 2C, D). Additionally, sperm nuclei were often seen in ectopic positions such as the uterus and near the vulva in *spe-19* hermaphrodites as they were swept from the spermatheca by passing oocytes (Fig. 2E).

To test whether or not hermaphrodite-derived sperm actually enter oocytes in *spe-19* animals, oocytes were dissected from the uterus and stained with DAPI. Although highly condensed sperm chromatin was clearly distinguishable from meiotically dividing chromatin in newly fertilized wild-type oocytes (Fig. 2F), no such sperm DNA was noted in the young oocytes of *spe-19* hermaphrodites (Fig. 2G). Older unfertilized *spe-19* oocytes contain the expected endomitotic DNA (Fig. 2H).

Taken together, the above results suggest a possible defect in sperm activation, as the full motility acquired with pseudopod generation during spermiogenesis is necessary for sperm migration, adherence to the spermatheca wall, prevention of displacement by passing oocytes and fertilization (Achanzar and Ward, 1997; Singson, 2001; Ward and Carrel, 1979; Zannoni et al., 2003).

spe-19 animals produce morphologically normal spermatids, but these fail to efficiently undergo activation in vitro

To further characterize *spe-19* spermatids, dissections were performed on male wild-type, *spe-19* and *spe-8* worms. Spermatids were examined using Nomarski imaging. Homozygous *spe-19* worms produced spermatids that were morphologically indistinguishable from either wild-type or *spe-8* worms (Figs. 3A–D).

spe-19 spermatids were treated in vitro with known sperm activators to assess their ability to undergo spermiogenesis (Nelson and Ward, 1980; Shakes and Ward, 1989b). When treated with Pronase, *spe-19* spermatids undergo activation less efficiently than wild-type (Table 1). Although a majority of *spe-19(hc41)* spermatids will eventually develop a pseudopod-like structure (82% vs. 97% in wild-type), they are typically shorter than wild-type, with an appearance similar to the aberrant pseudopods seen with activated *spe-8* and *spe-12* spermatids (Shakes and Ward, 1989a,b) (Figs. 3F–I, K–M). This failure to complete spermiogenesis is more pronounced in the *spe-19(eb52)* mutants (Table 1), with greater than 50% of spermatids arrested in the so-called "spiked" intermediate phase of spermiogenesis (MSP bundles project but fail to coalesce into a pseudopod) and only 32% progressing to maturity. In vitro activation experiments using the weak base TEA reveal a similar activation defect, with *spe-19(eb52)* spermatids arresting at the spiked intermediate stage of spermiogenesis (Fig. 3E), while *spe-8(hc40)* spermatids (known to undergo activation in TEA and used as a positive control) develop pseudopods (Fig. 3J). These results suggest that *spe-19* is a sperm activation mutant and that *spe-19(eb52)* is the more severe allele of the two.

Table 1
Quantification of sperm Pronase activation

Worm group	% Unactivated	% Arrest	% Activation
N2 (n = 74)	0	2.7	97.3
spe-19(eb52) (n = 136)	11.0	57.4	31.6
spe-19(hc41) (n = 85)	9.4	8.2	82.4

Virgin *spe-19* hermaphrodites were also dissected and their sperm examined using Nomarski imaging. Although they produced morphologically normal spermatids, no activated spermatozoa were noted (Fig. 3N), suggesting that *spe-19* hermaphrodite sperm are unable to undergo activation in vivo. Upon treatment with Pronase, *spe-19* hermaphrodite-derived spermatids behaved similarly to their male-derived counterparts, with many arresting at the spiked intermediate stage (Fig. 3O). These results suggest the sperm-loss phenotype described above is due to motility defects resulting from defective activation.

Mutations in spe-19 do not affect male fertility in vivo

Of the sperm activation genes known in *C. elegans*, the majority exhibit a hermaphrodite-specific phenotype (L'Hernault, 1997). To further address this issue in *spe-19*, we generated male lines for both *spe-19(eb52)* and *spe-19(hc41)* alleles.

To assess the effect of the *spe-19* mutation on male fertility, age-matched *spe-19* males were crossed to *dpy-5* hermaphrodites. Males were removed after 24 h and outcross progeny counted. There were no significant differences in brood sizes noted between *spe-19* alleles nor compared to wild-type (*eb52* = 215, *hc41* = 189, wild-type = 205) (Fig. 4A). We were also able to establish homozygous *spe-19* lines whose propagation is dependant on the presence of males.

It has been shown that wild-type *C. elegans* sperm engage in competition to fertilize oocytes and that male-derived sperm are competitively superior to hermaphrodite-derived sperm (Karr and Pitnick, 1999; LaMunyon and Ward, 1995, 1998). We therefore decided to test male-derived *spe-19* sperm by crossing homozygous *spe-19* males to *dpy-5* hermaphrodites and looking for a reduction in hermaphrodite self-fertility indicative of competition (Singson et al., 1999). Sperm from either *spe-19* allele engage in sperm competition with no

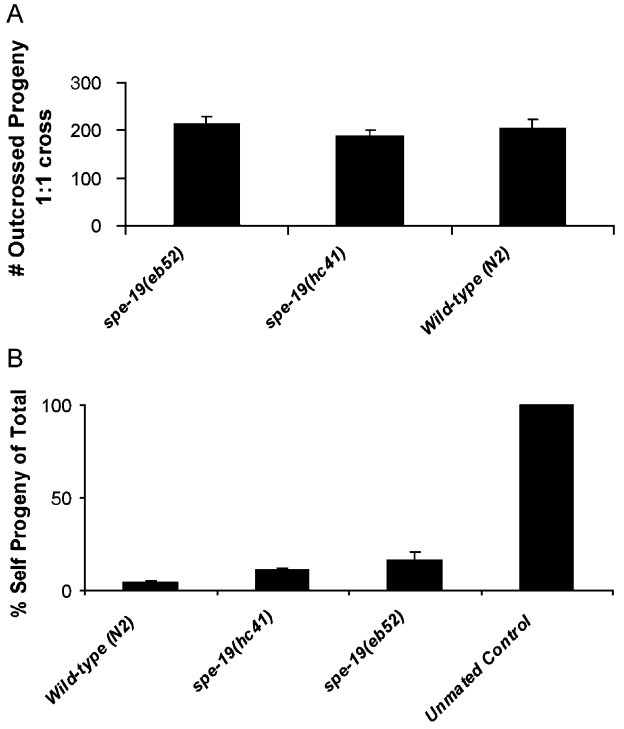

Fig. 4. *spe-19* male fertility. (A) Male fertility; *spe-19* males sire broods of comparable size to wild-type. Age-matched *spe-19* homozygous males were crossed into *dpy-5* hermaphrodites, removed after 24 h, and the number of outcross progeny scored. (B) Male fertility; *spe-19* males engage in sperm competition. Age-matched *spe-19* homozygous males were crossed into *dpy-5* hermaphrodites, removed after 24 h, and progeny were then examined. Unmated *dpy-5* and wild-type males were used as controls. $n > 15$ for all groups.

significant differences between alleles but less efficiently than wild-type (self progeny = 11% for *hc41*, 16% for *eb52* and 5% for wild-type ($P < 0.05$) (Fig. 4B). This ability to successfully compete with hermaphrodite-derived sperm suggests that male *spe-19* sperm undergo activation in vivo, are motile and can migrate to the recipient hermaphrodite's spermatheca.

Sperm from spe-19 animals exhibit little transactivation

Each of the four other known *spe-8* class mutants (*spe-8*, *spe-12*, *spe-27* and *spe-29*) exhibit a phenomenon termed transactivation whereby mutant hermaphrodite spermatids can form functional spermatozoa after exposure to male seminal fluid (LaMunyon and Ward, 1995; Singson et al., 1999). Transactivation ability varies among alleles; the greater the allele's severity, the lesser the transactivation. To determine whether *spe-19* hermaphrodites exhibit this behavior, we performed transactivation assays on both *spe-19* alleles using a temperature-sensitive allele of *fer-1*, whose male seminal fluid is known to be a potent transactivator for hermaphrodite spermatids (Table 2) (Shakes and Ward, 1989b). Homozygous *spe-19* hermaphrodites were crossed to *fer-1; him-5* homozygous males at 25°C, and the percentage of eggs to total ovulations was recorded. *spe-8(hc53)*, a hypomorphic sterile mutant known to exhibit robust transactivation behavior, was used as a positive control for *fer-1* seminal fluid activity. At this restrictive temperature, *fer-1* sperm are non-motile, and therefore no progeny would be expected unless seminal fluid is capable of activating hermaphrodite spermatids (Achanzar and Ward, 1997).

No significant differences between unmated *spe-19(eb52)* and *fer-1; him-5* × *spe-19(eb52)* animals were noted (the egg percentage of total ovulations = 0.24% for unmated *spe-19(eb52)* and 0.70% for *fer-1; him-5*-mated *spe-19(eb52)*). A small amount of transactivation was noted, however, between unmated *spe-19(hc41)* and *fer-1; him-5*-mated *spe-19(hc41)* (the egg percentage of total ovulations = .14% for unmated *spe-19(hc41)* and 3.85% for *fer-1; him-5*-mated *spe-19(hc41)* [$P = 0.00228$]).

To control for the success of copulation itself, we examined the fraction of hermaphrodites that produced fertilized eggs at all in both the unmated and *fer-1; him-5* mated groups. Significantly more mated *spe-8(hc53)* hermaphrodites laid eggs than did their unmated counterparts (5/20 unmated animals laid an average of 1.8 eggs each, while 14/19 mated animals laid an average of 72.1 eggs each [$P = 0.00616$]. Similarly, significantly more mated *spe-19(hc41)* hermaphrodites laid eggs than did their unmated counterparts (3/18 unmated worms laid an average of 1.3 eggs each, while 13/19 mated worms laid an average of 6.5 eggs each [$P = 0.00514$]). In the case of *spe-19(eb52)* hermaphrodites, there was no significant difference in the number of mated vs. unmated egg-laying worms (5/18 unmated *spe-19(eb52)* hermaphrodites laid an average of 1.2 eggs each, while 8/17 mated *spe-19(eb52)* worms laid an average of 2.6 eggs each). Thus, we cannot rule out the possibility that the lack of transactivation seen with the *spe-*

Table 2
spe-19 transactivation

Genotypes/crosses ($n > 15$ for all groups)	Average # eggs ± SEM	Average # oocytes ± SEM	Eggs as % of ovulation events
Unmated *spe-19(eb52)* hermaphrodite	0.3 ± 0.13	126.1 ± 18.019	0.24
fer-1(hc1) male × *spe-19(eb52)* hermaphrodite	1.05 ± 0.35	149.3 ± 17.733	0.70
Unmated *spe-19(hc41)* hermaphrodite	0.2 ± 0.12	138.95 ± 22.087	0.14
fer-1(hc1) male × *spe-19(hc41)* hermaphrodite	4.25 ± 1.35	106.2 ± 13.622	3.85
Unmated *spe-8(hc53);dpy-5(e61)* hermaphrodite	0.64 ± 0.27	17.29 ± 3.711	3.59
fer-1(hc1) male × *spe-8(hc53);dpy-5(e61)* hermaphrodite	46.45 ± 11.21	42.85 ± 7.668	52.02

19(eb52) allele is the result of unsuccessful mating rather than transactivation defects themselves. We believe this to be highly unlikely, however, as copulation was visually observed for all groups. Additionally, *spe-19(eb52)* hermaphrodites were subject to conditions identical to those of the *spe-19(hc41)* and *spe-8(hc53)* experiments where *fer-1* males did mate successfully.

These results are consistent with previously published transactivation results in other severe loss-of-function activation mutants and suggest both that our *spe-19* alleles are also strong loss-of-function and that *spe-19* is a key component for *C. elegans* sperm activation.

spe-19 sterility is suppressed by mutations in spe-6

It has recently been shown that the weak hypomorphic allele *spe-6(hc163)*, a gene previously known to play a role in Major Sperm Protein assembly, can also suppress sterility in the four hermaphrodite-specific activation genes *spe-8*, *spe-12*, *spe-27* and *spe-29*, bypassing the requirement for these genes in spermiogenesis (Muhlrad and Ward, 2002). To determine whether *spe-6(hc163)* could also obviate the need for the *spe-19* gene product, we constructed the *spe-6(hc163); spe-19(eb52)* double mutant and determined it to be fertile (see Materials and methods). This result strongly suggests that *spe-19* functions in the same genetic pathway as *spe-8*, *spe-12*, *spe-27* and *spe-29* and that *spe-19* functions upstream of *spe-6*.

Identification of the spe-19 gene

To determine the nature and function of the *spe-19* gene product, we cloned this gene employing a combination of two-point, three-point, deficiency and snip-SNP mapping. After localizing *spe-19* to the far right of chromosome V (Fig. 5A) within an approximately ~450 kb interval between two cosmids, we used a candidate gene approach. Of the 100 predicted genes within this interval, Y113G7A.10 appeared a likely prospect as it was

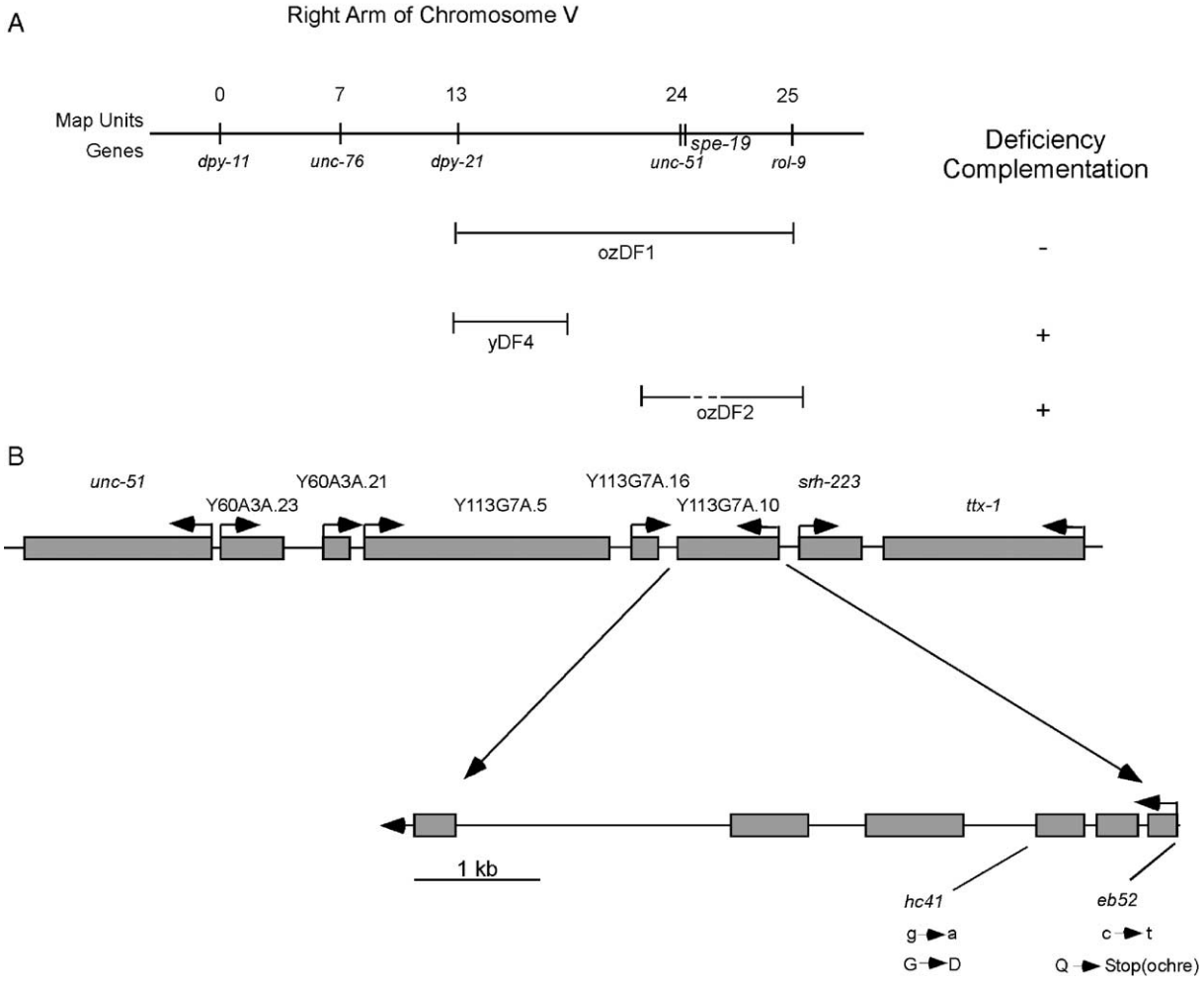

Fig. 5. The *spe-19* locus. (A) The right arm of chromosome V. The *spe-19* map position is shown. Regional deficiencies and complementation results are also indicated. (B) Graphical contextual representation of *spe-19*. Expanded view shows *spe-19* exon (boxes)/intron (lines) boundaries. The location of the mutation associated with each allele is indicated.

one of two genes in the region whose expression is sperm-enriched (Reinke et al., 2004).

We amplified a 7.3 kb fragment from wild-type worms containing Y113G7A.10 + ~850 bp of upstream sequence and assayed for its ability to rescue the sterility phenotype of *spe-19(eb52)* hermaphrodites. Of 36 injected worms, we recovered four stable rescuing lines. Two of these were then assayed for brood size to determine the extent of rescue (Fig. 1A). Although the transgene rescued fertility, brood sizes were less than those of wild-type worms, likely due to transgene germ line silencing (Putiri et al., 2004; Seydoux and Schedl, 2001).

Extrachromosomal arrays can often be lost, enabling the use of transgenic animals for mosaic analysis by assaying for our *myo3::gfp* transgene marker expression in the *spe-19* mutant background (Herman, 1995). Non-mosaic animals behaved as expected. Self-fertile transgene-containing *spe-19* hermaphrodites always transmitted the transgene through the germ line to the next generation (96/96). Animals of this genotype allowed us to propagate homozygous *spe-19* strains balanced by the transgene independent of the presence of males. When these animals are crossed to wild-type males (n = 4), we were able to obtain glowing male progeny, indicating that the transgenic array can be

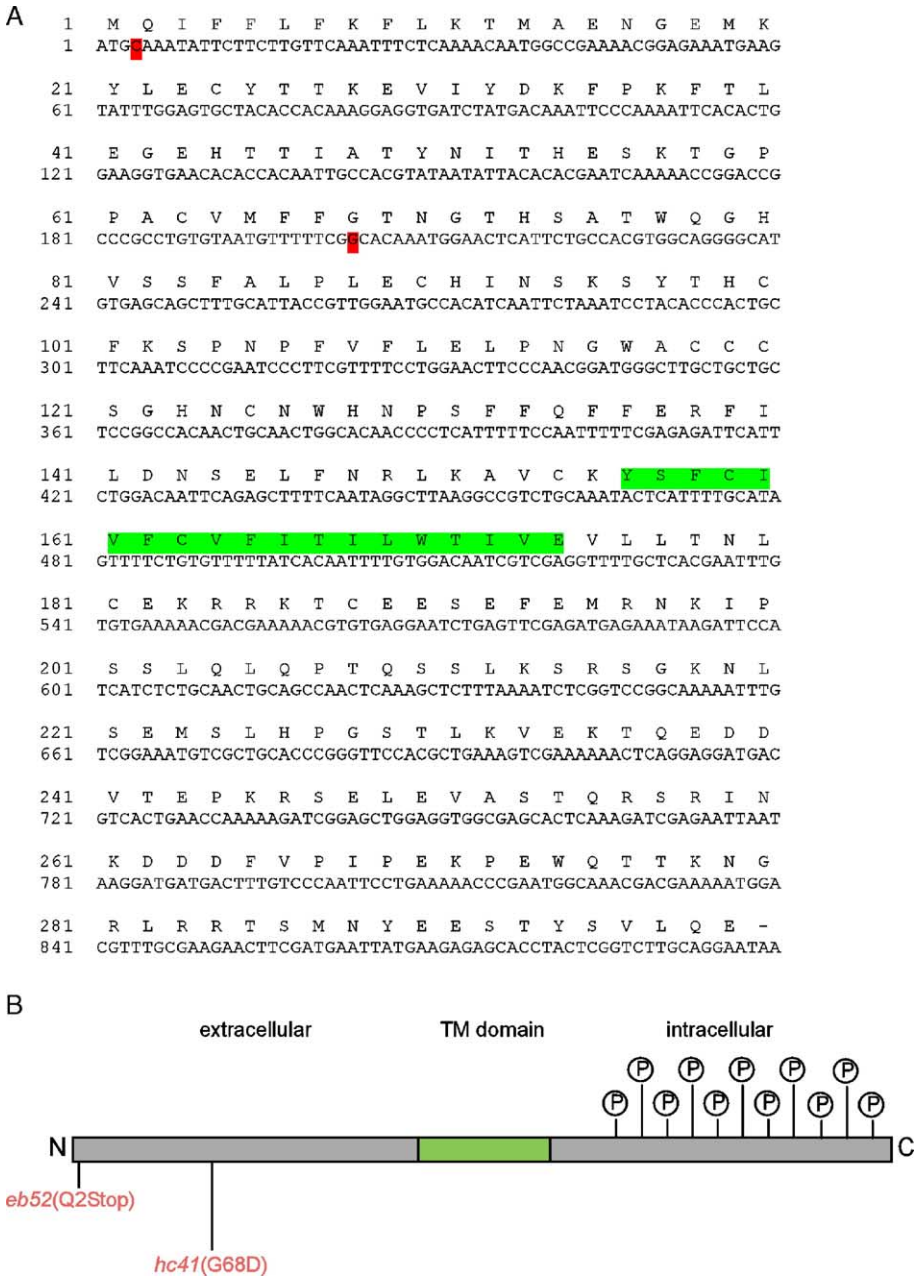

Fig. 6. *spe-19* sequence and mutations. (A) *spe-19* nucleotide and amino acid sequence. Bases mutated in each *spe-19* allele are highlighted in red, and the predicted transmembrane sequence is highlighted in green. (B) *spe-19* schematic. Orientation and position of TM domain are shown in the figure. Additionally, predicted phosphorylation sites are indicated.

transmitted through oocytes. In contrast, no self-sterile non-glowing *spe-19* hermaphrodite transmitted the rescuing transgene when mated to fertile homozygous *spe-19* males to produce F_1 progeny (264/264). Mosaic animals were also observed. Glowing Spe animals were checked for germ line transgene expression (n = 5) by crossing to homozygous *spe-19* males. All F_1 progeny were both Spe and non-glowing, indicating the F_0s did not carry the transgene in the germ line. We observed mosaic glowing self-fertile worms that sired glowing progeny (n > 20). We also observed rare non-glowing fertile worms (n = 3) that sired glowing progeny. These results suggest that *spe-19* is required in the germ line for fertility. While this mosaic analysis is not of sufficient resolution to rule out the possibility that the transgene is additionally required in some somatic tissue, *spe-19*'s sperm-enriched expression and sperm-specific mutant phenotype suggests this is unlikely.

Y113G7A.10 cDNA sequences were amplified from a male-derived cDNA library (Achanzar and Ward, 1997) and compared to genomic DNA to confirm/correct exon–intron boundaries. *spe-19* is composed of six small exons and five introns (Fig. 5B). To determine the molecular nature of the *spe-19* mutations, *spe-19* DNA was amplified from separate pooled lysates of *spe-19(eb52)*, *spe-19(hc41)* and wild-type animals, and all DNA was sequenced on both strands to ensure accuracy. *spe-19(hc41)* was found to contain a G to A transition in exon 3 that causes a G68 to D missense mutation. *spe-19(eb52)* was found to contain a C to T transition in exon 1 causing a Q2 to Stop (ochre) nonsense mutation. These mutations are consistent with those typical of EMS mutagenesis (Anderson, 1995). That *spe-19(eb52)* likely represents a genetic null is also consistent with the observation that it is the more severe loss-of-function allele.

The spe-19 gene product

The *spe-19* gene encodes a predicted 300 amino acid polypeptide (Fig. 6A) with no significant similarity to any other gene products in available databases excluding a single hypothetical ortholog in *C. briggsae* with which it shares 48% identity. Searches for conserved domains and motifs using Prosite (Gasteiger et al., 2003; Hulo et al., 2004), CCD (Marchler-Bauer et al., 2002; 2003) and CDART (Geer et al., 2002) produced no significant matches. Hydropathy analysis using TMPRED (Hofmann and Stoffel, 1993) suggests a single transmembrane domain with type 1 orientation (Fig. 6B). NetPhos analysis suggests at least 11 high-probability phosphorylation sites in the predicted intracellular portion of SPE-19 (Fig. 6B) (Blom et al., 1999).

Discussion

We report here on the identification and characterization of *spe-19*, a gene involved in spermiogenesis in *C. elegans* that shares a phenotype with four other genes known to be involved in the process: *spe-8*, *spe-12*, *spe-27* and *spe-29*. As with these genes, *spe-19* animals produce morphologically normal spermatids that fail to efficiently undergo activation, causing sperm motility defects, premature sperm depletion and sterility in hermaphrodites. Conversely, the effects of *spe-19* mutations on males are only detected with in vitro sperm activation; *spe-19* males are not only fertile, they engage in sperm competition and sire broods comparable in number to those of wild-type males.

The two alleles of *spe-19* differ in the nature of their mutations and in the severity of their effects. The mutations themselves are consistent with the types usually generated by EMS mutagenesis and are also consistent with differences in severity of the two alleles. *spe-19(hc41)* was found to contain a missense mutation in exon 3, resulting in the less severe loss-of function allele of the two. *spe-19(eb52)* contains a nonsense mutation in exon 1 and is likely to be a genetic null. Although the stop codon occurs so early it is possible that a downstream initiation codon might be used instead, the severe defects seen in *eb52* animals suggest this is unlikely.

The lower ovulation levels seen in *spe-19(eb52)* animals as compared to *spe-19(hc41)* or wild-type animals likely reflect their more severe sperm activation defects. As previously mentioned, spermatids are required to induce high levels of ovulation in *C. elegans* (McCarter et al., 1999; Miller et al., 2001). The more severe activation defects of *spe-19(eb52)* animals result in more pronounced spermathecal sperm loss ("sperm sweep") than in *spe-19(hc41)* animals and would be expected to result in a reduction (both physical and temporal) of any sperm signal/factor required for ovulation above basal levels.

Previous studies have demonstrated that both male- and hermaphrodite-derived spermatids can undergo activation to form functional spermatozoa after mating, a process termed transactivation (L'Hernault, 1997; Shakes and Ward, 1989b). In *spe-19* animals, transactivation occurs either poorly (*hc41*—an apparently severe hypomorph) or essentially not at all (*eb52*—an apparent genetic null) since the number of progeny produced after *fer-1* mating is less than the typical number of hermaphrodite spermatids present. These results suggest that no transactivation is the null phenotype and that hermaphrodite-derived sperm are themselves defective in the ability to undergo activation after mating. *spe-19*'s transactivation defect is comparable in severity to nulls of the other *spe* genes that are known to affect the process (*spe-8, spe-12*), suggesting *spe-19* to be an equally critical component for sperm activation (Minniti et al., 1996; Nance et al., 1999, 2000; Shakes and Ward, 1989b).

The question as to why male-derived activation-mutant spermatids such as *spe-19* can undergo spermiogenesis while hermaphrodite-derived ones do not is important. One possibility is that male and hermaphrodite activators are chemically identical, and males simply respond more

efficiently. Sperm activation presumably evolved coupled to male ejaculation (i.e. exposure to seminal fluid). Since hermaphrodism in *C. elegans* is believed to have been derived from an ancestral gonochoristic state (Cho et al., 2004; Kiontke et al., 2004), females must first have had to evolve to make spermatids and subsequently evolve a way to activate them. Thus, although they may use the same activator(s) as males, *C. elegans* hermaphrodites may be utilizing a less efficient endogenous spermatid activation pathway simply because they have had a shorter evolutionary history with spermatid activation. Additionally, while male-derived spermatids need to activate quickly before being swept out of the reproductive tract by passing eggs, hermaphrodite-derived sperm are synthesized prior to oogenesis. Consequently, hermaphrodites may be under less pressure for fast/robust spermatid activation than males. While perhaps of no practical consequence for a wild-type adult, this inherently lower hermaphrodite efficiency could become problematic in an activation-crippled mutant such as *spe-19*. This would also help to explain the transactivation behavior of sperm activation mutants, as transactivation effectively represents an uncoupling of ejaculation and activation, perhaps leading to a dosage or threshold effect in hermaphrodites. Whereas, in males, spermatids are co-ejaculated with seminal fluid, this is not the case with hermaphrodites. The increased exposure to seminal fluid likely results in an increase in both activator exposure and concentration, which may serve to increase activation efficiency in the male. Another possibility that cannot yet be ruled out is that male and hermaphrodite spermatids simply respond to different activators. More work will be needed to address this issue.

Prior evidence suggests that *spe-8*, *spe-12*, *spe-27*, *spe-29* and *spe-6* act in a common pathway and may function together in a multi-component complex (Muhlrad and Ward, 2002; Nance et al., 1999, 2000). The *spe-19* sterility suppression by *spe-6* (this study) strongly suggests that *spe-19* also acts in that pathway, upstream of *spe-6*. The severe activation defect of *spe-19* spermatids in vitro after exposure to proteases suggests that SPE-19 is likely not acting as an exogenous activator or required for activator synthesis or delivery. Instead, its large size and predicted single internal transmembrane domain suggest that SPE-19 is more likely involved in the reception/transduction of activator signals. The idea of SPE-19 as signal transducer is also supported by the size and localization of the other SPE activation proteins, all of which but the cytoplasmic kinase SPE-8 (Muhlrad and Ward, personal communication) are novel. SPE-12 is localized to the cell surface (Nance et al., 1999) and does not span the membrane, and SPE-27 is mostly hydrophilic with no extended regions of hydrophobicity (Minniti et al., 1996). While SPE-29 is a predicted transmembrane protein (Nance et al., 1999, 2000), its small size makes it a less likely candidate for the activation signal

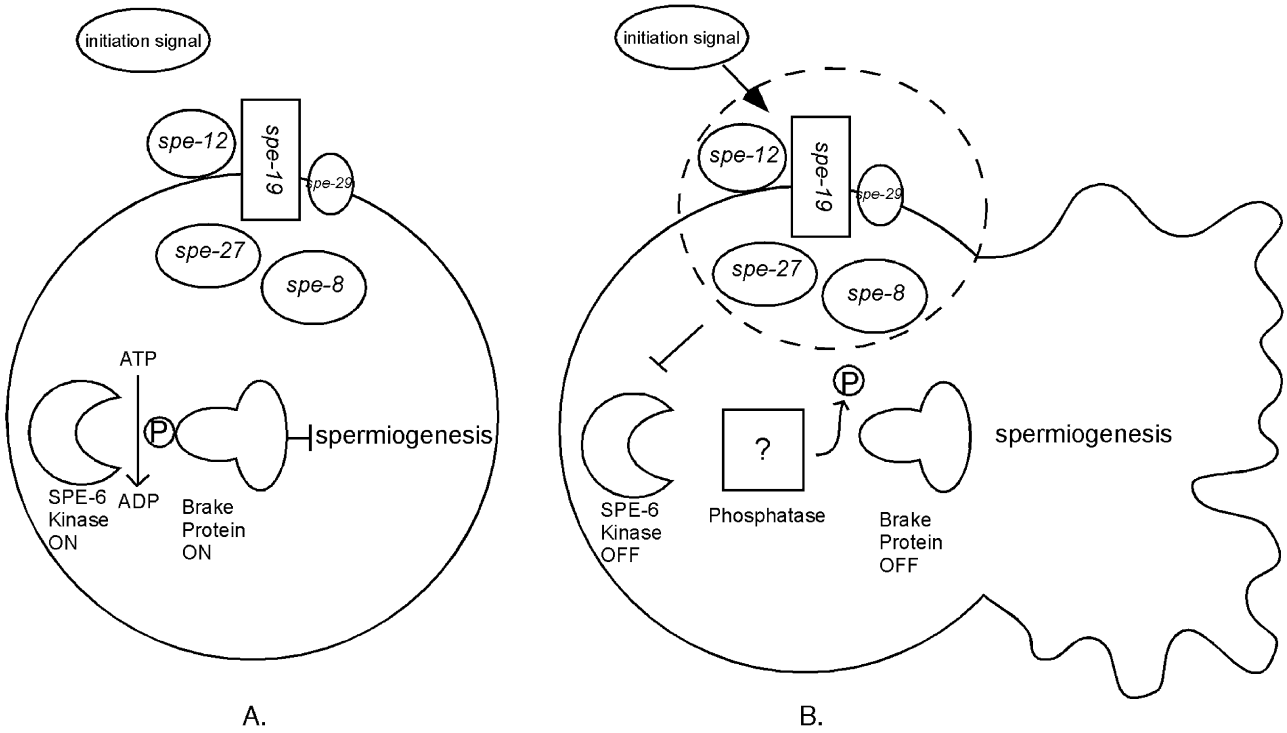

Fig. 7. Current model for sperm activation in *C. elegans*. (A) Unactivated spermatid. In the absence of a currently unidentified protease activator, a postulated intracellular brake protein keeps spermiogenesis in check via its phosphorylation by the casein kinase-like protein SPE-6. (B) Activated spermatozoa. The availability of the protease activator leads to the transduction of the initiation signal via a signaling complex that includes SPE-12, SPE-29 and SPE-19 at the plasma membrane and SPE-8 and SPE-27 in the cytoplasm. This signal serves to repress SPE-6 kinase activity, thereby releasing activation inhibition and allowing spermiogenesis to proceed.

transducer than SPE-19 (although a heterodimeric transduction complex involving both is also a possibility). Furthermore, the large number of predicted serine/threonine phosphorylation sites on the putative intracellular portion of SPE-19 adds additional support, especially given that spermatids lack translational machinery and spermiogenesis regulation must therefore occur post-translationally. Among spermatogenesis-enriched genes, the numbers of kinases and phosphatases are much greater than random expectation (Reinke et al., 2000), further implicating phosphorylation as a prominent mechanism for regulatory control of the process.

Based on our analysis of *spe-19*, we propose the following modification to the model for sperm activation first proposed by Muhlrad and Ward (2002) (Fig. 7). In the unactivated spermatid, a postulated intracellular regulatory brake protein keeps spermiogenesis in check via its phosphorylation by the casein kinase SPE-6. The availability of currently unidentified activator(s) leads to the transduction of the initiation signal via a signaling complex that includes SPE-12, SPE-29 and SPE-19 at the plasma membrane and SPE-8 and SPE-27 in the cytoplasm. The signal transduced by this complex serves to repress SPE-6 kinase activity, thereby releasing activation inhibition and allowing spermiogenesis to proceed.

Although we have identified SPE-19 as an important component of the spermiogenesis pathway in *C. elegans*, there remain some unidentified components and missing details in the above model. For example, despite genetic evidence of the SPE-8 protein class functioning in the same signaling pathway, the physical interactions between these members, if any, are not known. Do the members form a complex to transduce activation signals required for spermiogenesis, and if so, what is the nature of this complex? This is an important avenue for further research and one that will require biochemical means to address.

Additionally, a clear understanding of a signaling pathway is impossible without a complete inventory of its component molecules, which we currently lack with regard to *C. elegans* spermiogenesis. To further elucidate this pathway, it will be necessary to look to other currently uncloned activation genes, e.g., *fer-15*, whose male/hermaphrodite activation defect (L'Hernault, 1997) suggests that it functions further along the pathway to spermiogenesis activation (perhaps as the postulated phosphatase).

Acknowledgments

We would like to thank Lisa Caiafa, Kim McKim, Rick Padgett, Tina Gumienny and members of the Singson Laboratory for helpful discussions, critical comments and advice. We also wish to thank Jacob Rubin for his assistance with genetic mapping. Finally, we would like to thank Mako Saito and Tim Schedl for the *spe-19(eb52)* allele. The Singson Laboratory is supported by grants from the NIH (R01GM63089-01), Johnson and Johnson (Discovery Award) and the Charles and Johanna Busch Biomedical Fund. Additionally, Brian Geldziler received funding from an NIH Biotechnology Training Grant (5T32GM08339). The Caenorhabditis Genetics Center provided some nematode strains and is funded by the NIH National Center for Research Resources (NCRR).

References

Achanzar, W.E., Ward, S., 1997. A nematode gene required for sperm vesicle fusion. J. Cell Sci. 110, 1073–1081.

Anderson, P., 1995. Mutagenesis. Methods Cell Biol. 48, 31–58.

Blau, H.M., 1992. Differentiation requires continuous active control. Annu. Rev. Biochem. 61, 1213–1230.

Blom, N., Gammeltoft, S., Brunak, S., 1999. Sequence and structure-based prediction of eukaryotic protein phosphorylation sites. J. Mol. Biol. 294, 1351–1362.

Brenner, S., 1974. The genetics of *Caenorhabditis elegans*. Genetics 77, 71–94.

Chandrasekhar, A., Ennis, H.L., Soll, D.R., 1992. Biological and molecular correlates between induced dedifferentiation and spore germination in *Dictyostelium*. Development 116, 417–425.

Cho, S., Jin, S.W., Cohen, A., Ellis, R.E., 2004. A phylogeny of *Caenorhabditis* reveals frequent loss of introns during nematode evolution. Genome Res. 14, 1207–1220.

Derenlau, D.A., 1987. Blood platelet shape change ABCs. Trends Biochem. Sci., 439–442.

Finney, R., Ellis, M., Langtimm, C., Rosen, E., Firtel, R., Soll, D.R., 1987. Gene regulation during dedifferentiation in *Dictyostelium discoideum*. Dev. Biol. 120, 561–576.

Garner, M.H., Garner, W.H., Gurd, F.R., 1974. Recognition of primary sequence variations among sperm whale myoglobin components with successive proteolysis procedures. J. Biol. Chem. 249, 1513–1518.

Gasteiger, E., Gattiker, A., Hoogland, C., Ivanyi, I., Appel, R.D., Bairoch, A., 2003. ExPASy: the proteomics server for in-depth protein knowledge and analysis. Nucleic Acids Res. 31, 3784–3788.

Geer, L.Y., Domrachev, M., Lipman, D.J., Bryant, S.H., 2002. CDART: protein homology by domain architecture. Genome Res. 12, 1619–1623.

Geldziler, B., Kadandale, P., Singson, A., 2004. Molecular genetic approaches to studying fertilization in model systems. Reproduction 127, 409–416.

Herman, R.K., 1995. Mosaic analysis. Methods Cell Biol. 48, 123–146.

Hodgkin, J., 1997. Appendix 1, Genetics. In: Riddle, D.L., Blumenthal, T., Meyer, B.J., Priess, J.R. (Eds.), *C. Elegans* II. Cold Spring Harbor Laboratory Press, Cold Spring Harbor, pp. 881–1048.

Hofmann, K., Stoffel, W., 1993. TMbase—A database of membrane spanning proteins segments. Biol. Chem., 166.

Hulo, N., Sigrist, C.J., Le Saux, V., Langendijk-Genevaux, P.S., Bordoli, L., Gattiker, A., De Castro, E., Bucher, P., Bairoch, A., 2004. Recent improvements to the PROSITE database. Nucleic Acids Res. 32, D134–D137 (Database issue).

Jakubowski, J., Kornfeld, K., 1999. A local, high-density, single-nucleotide polymorphism map used to clone *Caenorhabditis elegans cdf-1*. Genetics 153, 743–752.

Karr, T.L., Pitnick, S., 1999. Sperm competition: defining the rules of engagement. Curr. Biol. 9, R787–R790.

Kiontke, K., Gavin, N.P., Raynes, Y., Roehrig, C., Piano, F., Fitch, D.H., 2004. *Caenorhabditis* phylogeny predicts convergence of hermaphroditism and extensive intron loss. Proc. Natl. Acad. Sci. U. S. A. 101, 9003–9008.

Kraft, B., Chandrasekhar, A., Rotman, M., Klein, C., Soll, D.R., 1989.

Dictyostelium erasure mutant HI4 abnormally retains development-specific mRNAs during dedifferentiation. Dev. Biol. 136, 363–371.
LaMunyon, C.W., Ward, S., 1995. Sperm precedence in a hermaphroditic nematode *Caenorhabditis elegans* is due to competitive superiority of male sperm. Experientia 51, 817–823.
LaMunyon, C.W., Ward, S., 1998. Larger sperm outcompete smaller sperm in the nematode *Caenorhabditis elegans*. Proc. R. Soc., Ser. B 265, 1997–2002.
L'Hernault, S.W., 1997. Spermatogenesis. In: Riddle, D.L., Blumenthal, T., Meyer, B.J., Priess, J.R. (Eds.), *C. Elegans* II. Cold Spring Harbor Laboratory, Cold Spring Harbor, pp. 271–294.
L'Hernault, S.W., Singson, A., 2000. Developmental genetics of spermatogenesis in the nematode *Caenorhabditis elegans*. In: Goldberg, E. (Ed.), The Testis: From Stem Cell to Sperm Function, Serono Symposium USA. Springer-Verlag Inc, New York, pp. 109–119.
Marchler-Bauer, A., Panchenko, A.R., Shoemaker, B.A., Thiessen, P.A., Geer, L.Y., Bryant, S.H., 2002. CDD: a database of conserved domain alignments with links to domain three-dimensional structure. Nucleic Acids Res. 30, 281–283.
Marchler-Bauer, A., Anderson, J.B., DeWeese-Scott, C., Fedorova, N.D., Geer, L.Y., He, S., Hurwitz, D.I., Jackson, J.D., Jacobs, A.R., Lanczycki, C.J., Liebert, C.A., Liu, C., Madej, T., Marchler, G.H., Mazumder, R., Nikolskaya, A.N., Panchenko, A.R., Rao, B.S., Shoemaker, B.A., Simonyan, V., Song, J.S., Thiessen, P.A., Vasudevan, S., Wang, Y., Yamashita, R.A., Yin, J.J., Bryant, S.H., 2003. CDD: a curated Entrez database of conserved domain alignments. Nucleic Acids Res. 31, 383–387.
McCarter, J., Bartlett, B., Dang, T., Schedl, T., 1999. On the control of oocyte meiotic maturation and ovulation in *C. elegans*. Dev. Biol. 205, 111–128.
Mello, C., Fire, A., 1995. DNA transformation. Methods Cell Biol. 48, 451–482.
Miller, M.A., Nguyen, V.Q., Lee, M.H., Kosinski, M., Schedl, T., Caprioli, R.M., Greenstein, D., 2001. A sperm cytoskeletal protein that signals oocyte meiotic maturation and ovulation. Science 291, 2144–2147.
Minniti, A.N., Sadler, C., Ward, S., 1996. Genetic and molecular analysis of spe-27, a gene required for spermiogenesis in *Caenorhabditis elegans* hermaphrodites. Genetics 143, 213–223.
Muhlrad, P.J., Ward, S., 2002. Spermiogenesis initiation in *Caenorhabditis elegans* involves a casein kinase 1 encoded by the *spe-6* gene. Genetics 161, 143–155.
Nachmias, V.T., Yoshida, K., Glennon, M.C., 1987. Lowering pH in blood platelets dissociates myosin phosphorylation from shape change and myosin association with the cytoskeleton. J. Cell Biol. 105, 1761–1769.
Nance, J., Minniti, A.N., Sadler, C., Ward, S., 1999. spe-12 encodes a sperm cell surface protein that promotes spermiogenesis in *Caenorhabditis elegans*. Genetics 152, 209–220.
Nance, J., Davis, E.B., Ward, S., 2000. spe-29 encodes a small predicted membrane protein required for the initiation of sperm activation in *Caenorhabditis elegans*. Genetics 156, 1623–1633.
Nelson, G.A., Ward, S., 1980. Vesicle fusion, pseudopod extension and amoeboid motility are induced in nematode spermatids by the ionophore monensin. Cell 19, 457–464.
Primakoff, P., Myles, D.G., 2002. Penetration, adhesion, and fusion in mammalian sperm–egg interaction. Science 296, 2183–2185.
Putiri, E., Zannoni, S., Kadandale, P., Singson, A., 2004. Functional domains and temperature-sensitive mutations in SPE-9, an EGF repeat-containing protein required for fertility in *Caenorhabditis elegans*. Dev. Biol. 272, 448–459.
Reinke, V., Smith, H.E., Nance, J., Wang, J., Van Doren, C., Begley, R., Jones, S.J., Davis, E.B., Scherer, S., Ward, S., Kim, S.K., 2000. A global profile of germline gene expression in *C. elegans*. Mol. Cell 6, 605–616.
Reinke, V., Gil, I.S., Ward, S., Kazmer, K., 2004. Genome-wide germline-enriched and sex-biased expression profiles in *Caenorhabditis elegans*. Development 131, 311–323.
Seydoux, G., Schedl, T., 2001. The germline in *C. elegans*: origins, proliferation, and silencing. Int. Rev. Cytol. 203, 139–185.
Shakes, D., 1988. A Genetic and Pharmacological Analysis of Spermatogenesis in the Nematode *Caenorhabditis Elegans*. Biology Department. Johns Hopkins University, Baltimore, pp. 189.
Shakes, D., Ward, S., 1989a. Mutations that disrupt the morphogenesis and localization of a sperm-specific organelle in *Caenorhabditis elegans*. Dev. Biol. 134, 307–316.
Shakes, D.C., Ward, S., 1989b. Initiation of spermiogenesis in *C. elegans*: a pharmacological and genetic analysis. Dev. Biol. 134, 189–200.
Shapiro, L., 1985. Generation of polarity during Caulobacter cell differentiation. Annu. Rev. Cell Biol. 1, 173–207.
Simon, M.A., Bowtell, D.D., Dodson, G.S., Laverty, T.R., Rubin, G.M., 1991. Ras1 and a putative guanine nucleotide exchange factor perform crucial steps in signaling by the sevenless protein tyrosine kinase. Cell 67, 701–716.
Simons, K., Fuller, S.D., 1985. Cell surface polarity in epithelia. Annu. Rev. Cell Biol. 1, 243–288.
Simons, K., Wandinger-Ness, A., 1990. Polarized sorting in epithelia. Cell 62, 207–210.
Singson, A., 2001. Every sperm is sacred: fertilization in *Caenorhabditis elegans*. Dev. Biol. 230, 101–109.
Singson, A., Hill, K.L., L'Hernault, S.W., 1999. Sperm competition in the absence of fertilization in *Caenorhabditis elegans*. Genetics 152, 201–208.
Vacquier, V.D., 1975. The isolation of intact cortical granules from sea urchin eggs: calcium ions trigger granule discharge. Dev. Biol. 43, 62–74.
Ward, S., Carrel, J.S., 1979. Fertilization and sperm competition in the nematode *Caenorhabditis elegans*. Dev. Biol. 73, 304–321.
Wassarman, P.M., Jovine, L., Litscher, E.S., 2001. A profile of fertilization in mammals. Nat. Cell Biol. 3, E59–E64.
Zannoni, S., L'Hernault, S.W., Singson, A.W., 2003. Dynamic localization of SPE-9 in sperm: a protein required for sperm–oocyte interactions in *Caenorhabditis elegans*. BMC Dev. Biol. 3, 10.